

Light Trapping in Thin-Film Cu(InGa)Se₂ Solar Cells

James G. Mutitu, Uwadiae Obahiagbon, Shouyuan Shi, William Shafarman, and Dennis W. Prather

Abstract—A fundamental optical analysis of thin-film Cu(InGa)Se₂ solar cell structures is presented, wherein spectroscopic ellipsometry measurements were performed to acquire material optical constants, which were then used as input parameters to perform electromagnetic simulations. The accuracy of the electromagnetic simulation tools, and thus, the validity of the material optical constants, were verified by comparing the values determined from the simulations with experimental measurements obtained using a spectrophotometer. The verified optical modeling tools were then used to analyze thin, <0.7- μm Cu(InGa)Se₂ solar cell structures, which do not absorb all incident light within a single optical path length, and hence, the need to incorporate light trapping. To this end, a superstrate device configuration was employed in which the metallic back contact is deposited last, giving rise to an opportunity to incorporate photonic engineering device concepts to the back surface layer of the solar cell. Simulations of superstrate Cu(InGa)Se₂ solar cell designs, complete with light trapping structures were then performed and analyzed.

Index Terms—Diffraction, photovoltaic cells, solar energy.

I. INTRODUCTION

A GOOD understanding of the interaction between incident light and a solar cell device structure is critical to optimizing device performance. To this end, improving thin-film solar cell performance by increasing the light-trapping capacity has received significant attention in the recent past. Many of these studies have focused on c-Si and a-Si because of the ubiquitous use of these materials throughout the semiconductor industry, in addition to the emergence and growth of the silicon photonics industry [1]–[3]. In contrast, only a handful

Manuscript received July 11, 2013; revised September 20, 2013; accepted October 20, 2013. Date of publication March 14, 2014; date of current version April 18, 2014. This work was supported by the Department of Energy under Award DE-EE0005317. This report was prepared as an account of work sponsored by an agency of the United States Government. Neither the United States Government nor any agency thereof, nor any of their employees, makes any warranty, express or implied, or assumes any legal liability or responsibility for the accuracy, completeness, or usefulness of any information, apparatus, product, or process disclosed, or represents that its use would not infringe privately owned rights. Reference herein to any specific commercial product, process, or service by trade name, trademark, manufacturer, or otherwise does not necessarily constitute or imply its endorsement, recommendation, or favoring by the United States Government or any agency thereof. The views and opinions of authors expressed herein do not necessarily state or reflect those of the United States Government or any agency thereof.

J. G. Mutitu and U. Obahiagbon are with the Department of Electrical and Computer Engineering and the Institute of Energy Conversion, University of Delaware, Newark, DE 19716 USA (e-mail: mutitu@udel.edu; uwa@udel.edu).

S. Shi and D. W. Prather are with the Department of Electrical and Computer Engineering, University of Delaware, Newark, DE 19716 USA (e-mail: sshi@mail.eecis.udel.edu; dprather@mail.eecis.udel.edu).

W. Shafarman is with the Institute of Energy Conversion, University of Delaware, Newark, DE 19716 USA (e-mail: wns@udel.edu).

Color versions of one or more of the figures in this paper are available online at <http://ieeexplore.ieee.org>.

Digital Object Identifier 10.1109/JPHOTOV.2014.2307487

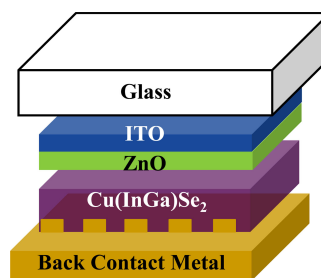


Fig. 1. Structure of the Cu(InGa)Se₂ superstrate design complete with diffraction gratings.

of groups have explored light trapping in Cu(InGa)Se₂ solar cells, due in part to its high absorption coefficient, which ensures that 95% of the incident illumination is absorbed within a 1- μm thick layer, i.e., within a wavelength band corresponding to the material bandgap. However, when the thickness of the Cu(InGa)Se₂ absorber layer is reduced to below 1 μm , a single optical pass of light through the material is insufficient to fully absorb as much light as compared with thicker cells, and thus, the need for incorporating light-trapping schemes arises. The advantages of having thin, <1- μm thick, Cu(InGa)Se₂ absorber layers include, reduced material costs and shorter device processing times, which ultimately lead to an increase in manufacturing throughput and lower capital requirements for deposition processes. In practice, however, the efficiency of superstrate devices still lags behind those of conventional substrate devices, which further serves to prove the need for light-trapping studies in thin Cu(InGa)Se₂ solar cells.

In the past, studies by Orgassa *et al.* examined the effects of a variety of metallic back contact reflectors on Cu(InGa)Se₂ light trapping [4]. Malmström *et al.* investigated the effects of a TiN back contact and reflector, in addition to front and back surface scattering [5]. However, many of these studies have been focused on substrate device configurations, where all the device components are deposited on top of a material substrate, e.g., soda lime glass.

Traditional substrate configurations of Cu(InGa)Se₂ solar cells present a major problem when it comes to light-trapping design. The main problem is that a substrate fabrication process requires that the choice of back contact material be inert, in order to withstand the highly corrosive environment that is generated during the Cu(InGa)Se₂ deposition step. This limits greatly the choices of available back surface materials. To circumvent this hurdle, a superstrate design configuration is utilized, whereby the constituent solar cell materials are deposited in the order of ITO/ZnO/Cu(InGa)Se₂/metal back contact, onto a glass superstrate, as shown in Fig. 1.

The superstrate configuration enables a thinner absorber layer and overcomes the inert metal constraint, which affects

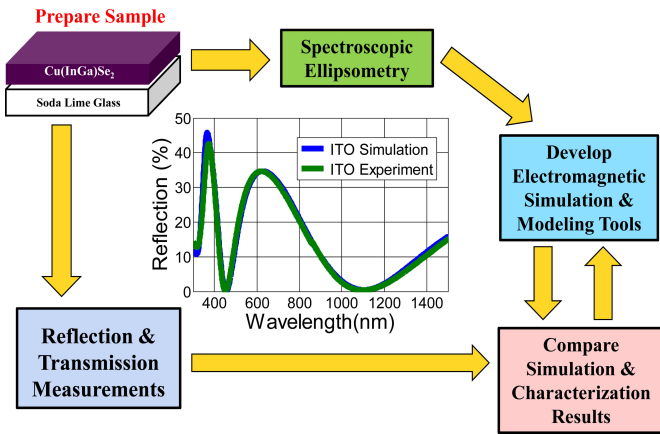


Fig. 2. Integrated Loop approach used to verify optical material characteristics and accuracy of simulation tools. (Inset) Example of the comparison between the simulation and experimental data from ITO.

traditional substrate devices, since the back contact is deposited after the Cu(InGa)Se₂ layer has been deposited. Additional advantages of superstrate solar cells include: the elimination of the need for a glass back sheet, which leads to lower cost and lighter weight modules; greater flexibility and simplification in the laser scribing process, which is ultimately necessary for monolithic integration; and finally, the ability to process the TCO layers at elevated temperatures, which leads to improved reliability and performance.

II. OVERVIEW

This paper focuses on building a fundamental framework for the study of light-trapping techniques in superstrate configured Cu(InGa)Se₂ solar cells. The goal is to develop a reliable electromagnetic simulation tool that can be used to optimize various design parameters in Cu(InGa)Se₂ solar cells, such as layer thicknesses, and thus, design better performing devices. To accomplish this, a customized integrated loop approach is employed, whereby samples are prepared and analyzed through two distinct methods, the first being ellipsometry, which gives material optical constants that can then be used to develop the electromagnetic modeling tools. The second method utilizes a spectrophotometer to take alternate measurements that can then be directly compared with the output of the electromagnetic models, thereby verifying the validity of the simulations, as is shown in Fig. 2.

The first step in the integrated loop process is to accurately obtain the optical constants of materials in order to ensure that the subsequent analyses—including the development of simulation tools—are of the highest accuracy. To achieve the desired precision in analysis, there is a strong need to be able to deposit repeatable material compositions and then analyze them using variable angle spectroscopic ellipsometry (VASE) measurements. The second step requires that the deposited samples be prepared, which could entail the need for material etches to smoothen surfaces, in order to obtain reliable instrument readings during the VASE analysis. The VASE analysis, in turn, calls for the modeling of material properties using dispersion

equations to obtain the optical constants, which is not a trivial process. In addition, some material systems consist of complex compositional gradients, and hence, exhibit inhomogeneous refractive index profiles. To this end, the optical characterization using VASE may in some cases be used to obtain average, or bulk, material refractive index values. Similarly, it may also be impossible to completely represent the physical structure of a solar cell device using simulation software, especially in situations where a considerable amount of surface roughness is present, and again such situations may call for the use of some approximations. However, to circumvent the accumulation of many erroneous results, further characterization is required. In this case, a spectrophotometer is used; the results obtained from spectrophotometer measurements can be directly compared with simulation results, and hence, provide a reliable means by which to ascertain the veracity of both the VASE characterization and simulation processes. The verified computational tools can thereafter be used to design complex light-trapping structures, such as the one shown in Fig. 1.

III. EXPERIMENTAL METHODS

The Cu(InGa)Se₂ films were deposited using an elemental coevaporation of Cu, In, Ga, and Se from independent sources in a Belljar evaporator system at a substrate temperature of 550 °C. A single-stage deposition recipe was used, whereby all the fluxes, of all the constituent materials, were held constant throughout the process, producing films with uniform compositions and no Ga gradient [6]–[8]. The resulting films were $\sim 2\text{-}\mu\text{m}$ thick films with a [Cu]/[In+Ga] composition of about 0.9 and a [Ga]/[In+Ga] composition of 0.3, giving rise to a bandgap of 1.2 eV. This coevaporation process produces a film with a high amount of surface roughness, which makes it difficult to acquire accurate optical constants. To circumvent this hurdle, Paulson *et al.*, peeled off the Cu(InGa)Se₂ film by exploiting the weakness that occurs at the MoSe₂ layer between the Cu(InGa)Se₂ and Mo layers [8], [9]. Shafarman *et al.* also determined the optical constants of Cu(InGa)Se₂ by first reducing the roughness and then removing residual Se on the surface using a Br-etch and KCN etch, respectively [7]. In this study, the latter technique was employed using the optimized Br and KCN etch processes. It is worthy to note that, typical values of root-mean-square (rms) roughness measured by atomic force microscopy on Cu(InGa)Se₂ films are between 50 and 100 nm making it difficult to make valid ellipsometry measurements. The rms surface roughness is reduced by the Br-Etch process to less than 10–15 nm, which is significantly smaller than the incident ellipsometer beam wavelengths, and hence, does not adversely affect the measurements [10], [11].

Thin films of ZnO and ITO with thicknesses of 162 nm and 92 nm, respectively, were deposited using a sputtering process; the resultant layers had sheet resistances of $5 \times 10^3 \Omega/\square$ (for ZnO) and $12.1 \Omega/\square$ (for the ITO). A 200-nm gold layer was deposited using electron beam evaporation, and a similar process was used to produce a 500-nm silver layer. Optical constants of these individual films were obtained using a J. A. Woolam rotating analyzer variable spectroscopic ellipsometer that is

equipped with an autoretarder. The VASE instrument works by measuring the change in polarization that light waves experience as they are reflected from surfaces and interfaces through planar multilayered materials [12], [13]. The VASE measurements yield a phase difference (Δ) and an amplitude ratio (ρ), which is the complex reflectance ratio of the parallel (r_p) and perpendicular (r_s) wave polarizations, based on the Fresnel equations for reflection and transmission. The complex reflectance ratio (ρ) used in VASE is measured as function of both angle and wavelength. The relationship between all these terms is shown in

$$\tan(\Psi)e^{i\Delta} = \rho = \frac{r_p}{r_s} \quad (1)$$

where $\tan(\Psi)$ represents the amplitude ratio of the reflected waves (magnitude of reflectance ratio, ρ).

Since VASE measures the complex ratio between two values it can be highly accurate in addition to yielding phase information; the self-referencing nature of the measurement ensures that the effects of fluctuations in lamp intensity, or degradation, do not affect the final results, and hence, the measurements are reproducible.

The reflectance and transmission measurements were acquired using a Perkin–Elmer Lambda 750 spectrophotometer, fitted with an integrating sphere. The spectrophotometer normalizes the results of reflectance and transmission measurements to those achieved using calibrated reflectance standards.

IV. OPTICAL CONSTANT VERIFICATION

Throughout the optical characterization process, a number of issues arose. Initially, each material was deposited on a soda-lime glass (SLG) substrate and then analyzed using VASE. It would appear that obtaining the refractive index of a glass substrate, such as SLG should be a straightforward process. However, it turns out that during the Pilkington glass manufacturing process some of the molten tin, on which the glass floats, diffuses into the glass, giving rise to the tin or float side of the SLG [14]. This tin side creates a nonlinear graded refractive index profile, which extends about 900 nm into the 1.6-mm-thick SLG. In addition, the bulk of SLG exhibits birefringence, i.e., the refractive index depends on the polarization and propagation direction of light. The air side also has a different refractive index [14]. This complexity associated with the SLG analysis led to a substitution of c-Si substrates for the ITO and ZnO layers. Crystalline silicon is a well understood material that exhibits a large refractive index contrast between it and ITO or ZnO. Using the c-Si substrate led to the acquisition of lower mean square error values during the VASE analysis, which were 5.4 and 3.8 for the ITO and ZnO films, respectively. The ZnO layer was modeled using a General Oscillator model, which allows for the combination of multiple oscillator models, in this case a P-Semi and Gaussian oscillator were used; the General Oscillator model is one of the dispersion formulae that is released by the J. A. Woollam Company in their CompleteEASE software package, which is used to create the ellipsometer models [15]. The ITO was modeled using a B-Spline dispersion layer, which is a dispersion equation based on the B-Spline recursion relation and is consistent with Kramers–

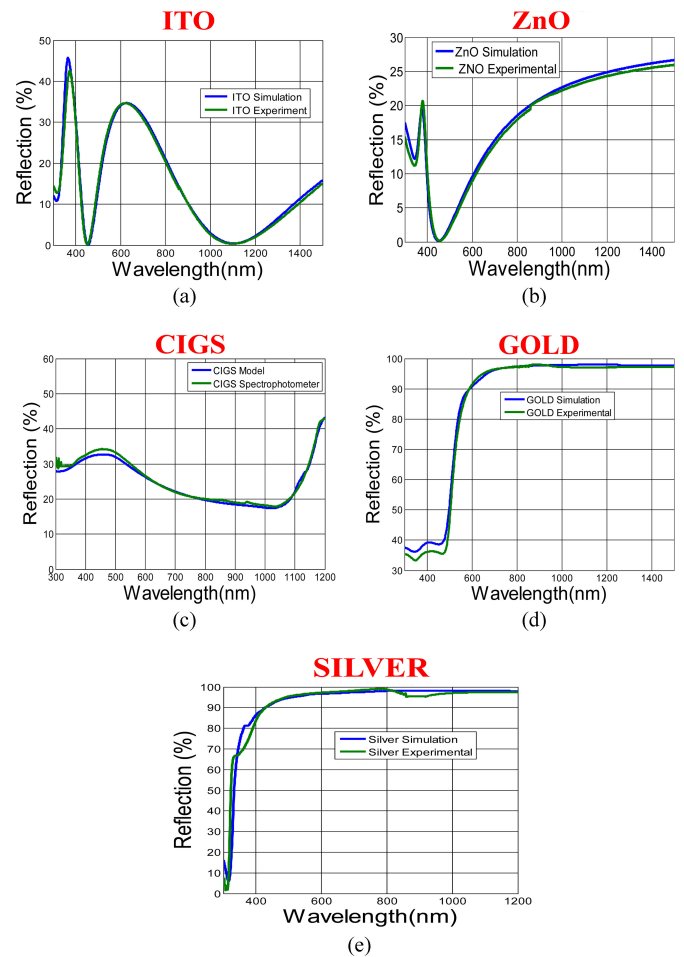


Fig. 3. Comparison between experimental and simulated reflectance for (a) ITO, (b) ZnO, (c) Cu(InGa)Se₂, (d) Gold, and (e) Silver.

Kronig relations [16], even though a free carrier Drude model combined with a Lorenz oscillator could also have been used. The gold layer was modeled using a B-Spline layer, which gave an MSE of about 2 [16], whereas with silver, the values were retrieved from the DeltaPsi2 software—from Horiba—based on modified data values obtained from the text *Handbook of optical constants of solids* by E. Palik [17], [18]. The comparison between experimental data, obtained from spectrophotometer measurements, and simulation data is shown in Fig. 3.

Throughout this study with Cu(InGa)Se₂, it was found that the material may have a graded index profile, depending on how the deposition process actually occurred. Nevertheless, with multiple measurements, such as spectroscopic transmission intensity measurements—performed on a Cu(InGa)Se₂ layer on an SLG substrate—which could be modeled simultaneously with data from more traditional VASE reflectance measurements, it was possible to obtain better complex refractive index values. The Cu(InGa)Se₂ was modeled using a B-Spline layer. Additional ellipsometry, simulations and spectrophotometer characterizations were performed on a Cu(InGa)Se₂ layer deposited on a crystalline silicon substrate. The resultant simulation data also matched up well with experimental data, as is shown in Fig. 3(c).

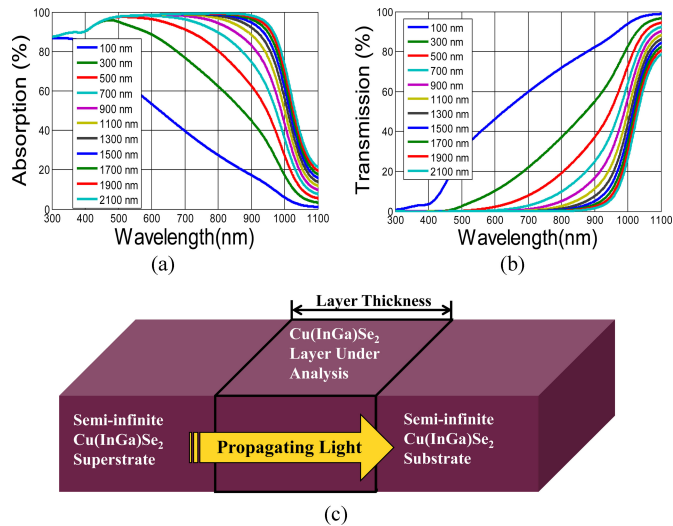


Fig. 4. (a) Absorption and (b) transmission characteristics of $\text{Cu}(\text{InGa})\text{Se}_2$ layers of various thicknesses. (c) $\text{Cu}(\text{InGa})\text{Se}_2$ layers that are under analysis, in (a) and (b), are sandwiched between two semiinfinite structures of the same material, and therefore, no front or back surface reflections occur. A light wave propagating through the layer of interest is also shown.

All the other materials properties used in this light-trapping study were obtained from previous studies [3], [8]–[10].

The electromagnetic simulation tool that was used throughout this study is centered on the scattering matrix algorithm, which is a modified version of a transfer matrix-based algorithm that is used to solve Maxwell's equations rigorously for each individual wavelength in the spectrum being considered [20]–[22]. In this algorithm, the structure to be simulated is broken up into many individual layers in the direction of light illumination. The fields in each layer are expanded into Fourier modes, whereby redundant Fourier modes are also incorporated in order to ensure the accuracy of the scattering matrix method; this also includes cases where large index contrast materials are considered. The expansion coefficients for each Fourier mode are then used to form the scattering matrix. The scattering matrices from each of the layers are then cascaded in order to attain an overall system matrix that can be used to provide both reflection and transmission characteristics. The application of periodic boundary conditions makes it possible to significantly reduce the computation time, thus making the S-Matrix method suitable for thin-film solar cell applications.

V. FUNDAMENTAL LIGHT-TRAPPING STUDY

In order to perform a light-trapping study of value, it is necessary to identify the optical characteristics of a material when no optical enhancements or reflections occur. This is calculated by placing the $\text{Cu}(\text{InGa})\text{Se}_2$ between two semiinfinite structures of the same material, i.e., a superstrate and substrate of $\text{Cu}(\text{InGa})\text{Se}_2$ in this case, and letting light flow from within the superstrate, through the structure and out into the substrate, as shown in Fig. 4(c). This way, it is possible to determine how much light is absorbed within a certain thickness of the material. This type of analysis was performed on $\text{Cu}(\text{InGa})\text{Se}_2$ layers with thicknesses ranging from 100 to 2100 nm with a 200-nm

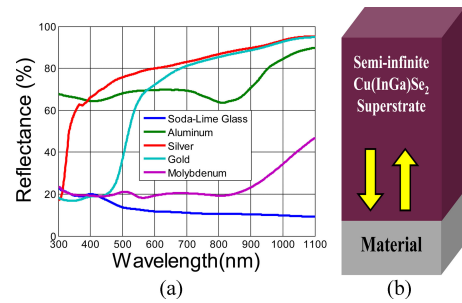


Fig. 5. (a) Reflectance characteristics of different back surface materials into a semiinfinite $\text{Cu}(\text{InGa})\text{Se}_2$ structure and (b) illustration of the structure under analysis for each material shown in (a).

interval, using the optical constants that had been previously obtained using the integrated loop analysis process, and the results are plotted in Fig. 4(a) and (b).

This exercise enabled the observation of the absorption characteristics of light in a single optical path length. The wavelength range of this analysis was limited to 300–1100 nm, which corresponded to the bandgap of the coevaporated $\text{Cu}(\text{InGa})\text{Se}_2$, which is about 1.2 eV [6]–[9]. As can be seen in Fig. 4(b), for a structure that is 700-nm thick, only light of wavelengths above 600 nm would hit the back reflector surface, and hence, that is the range where the back reflector design is focused.

The reflectance characteristics were simulated for different back surface materials, including soda-lime glass, aluminum, silver, gold, and molybdenum, with each of these materials placed below a semiinfinite layer of $\text{Cu}(\text{InGa})\text{Se}_2$. As can be seen in Fig. 5, gold and silver exhibited the best reflectance characteristics especially at longer wavelength regions. Molybdenum, which is the commonly used back contact for $\text{Cu}(\text{InGa})\text{Se}_2$ solar cells, did not exhibit good reflectance characteristics.

An optimization of the thicknesses of the ITO and ZnO layers was performed using the particle swarm optimization algorithm [3] to reduce the device reflectance. It is pertinent to note that the soda-lime glass in this case was treated as a semiinfinite superstrate, so as to focus on the ITO and ZnO thicknesses specifically. The optimal design parameters were found to be 150 nm of ITO and 112 nm of ZnO, which gave an average reflectance of 6.5% in the 300–1100 nm range.

Finally, the optimized ITO and ZnO coatings, along with the silver or gold back reflectors, were applied to a superstrate solar cell with 0.7- μm thick $\text{Cu}(\text{InGa})\text{Se}_2$ —in a structure similar to Fig. 1 but without the diffraction gratings—and the light-trapping characteristics were simulated. An additional diffraction grating, with a period of 860 nm and 50% fill factor (similar to Fig. 1)—corresponding to feature sizes that have previously been realized using a deep ultraviolet lithography process [19]—was included to the final design structure and simulated. The resultant absorption characteristics of the different structures are plotted in Fig. 6. It was observed that the absorption characteristics were almost the same, which is what was expected, considering that the reflectance of gold and silver, into $\text{Cu}(\text{InGa})\text{Se}_2$, is almost identical for wavelengths above 750 nm, as was shown in Fig. 5. Additionally, all wavelengths below 750 nm would be absorbed in the 700-nm $\text{Cu}(\text{InGa})\text{Se}_2$ layer

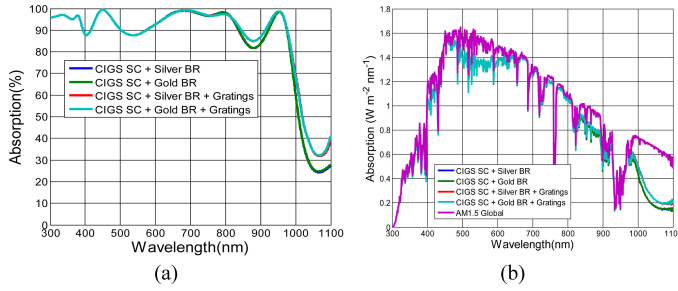


Fig. 6. (a) Percentage and (b) total power absorption characteristics of 700-nm-thick $\text{Cu}(\text{InGa})\text{Se}_2$ solar cell structures with various optical enhancements; silver and gold back reflectors and silver and gold diffraction gratings.

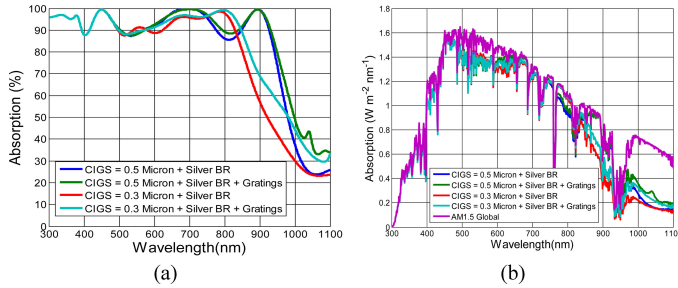


Fig. 7. (a) Percentage and (b) total power absorption characteristics of 300- and 50-nm $\text{Cu}(\text{InGa})\text{Se}_2$ solar cell structures with various optical enhancements; silver back reflectors and silver diffraction gratings.

TABLE I
OPTIMAL DESIGN PARAMETERS OF MATERIALS USED IN $\text{Cu}(\text{InGa})\text{Se}_2$ SOLAR CELL STRUCTURE SIMULATIONS

Material	Thickness (nm)
ITO	150
ZnO	112
$\text{Cu}(\text{InGa})\text{Se}_2$	300/500/700
Grating Thickness	150
Grating Period	860
Back Metal	1000

before ever reaching the back reflector, as can be inferred from Fig. 4.

It was finally decided that silver be used for the rest of the study because of its wider bandwidth of high reflectance, when compared with gold, which would work better for thinner $\text{Cu}(\text{InGa})\text{Se}_2$ structures; this conclusion was derived from observing the reflectance graphs in Fig. 5(a).

The same optimized design parameters, as used in the structures of Fig. 6, were applied to thinner, i.e., 0.5- and 0.3- μm -thick $\text{Cu}(\text{InGa})\text{Se}_2$, solar cell structures, but this time only utilizing silver as the back surface and diffraction grating material, and the results are plotted in Fig. 7.

As can be seen in Fig. 7, the structures with the silver diffraction gratings outperformed the other structures, of corresponding thickness, which only had a planar reflector.

The optimal design parameters used for the simulation results of Figs. 6 and 7, are summarized in Table I.

The absorption characteristics, in terms of averaged percentage and total power absorbed, for all the simulation results presented in Figs. 6 and 7 are summarized in Table II.

TABLE II
ABSORPTION CHARACTERISTICS FOR ALL THE SIMULATED $\text{Cu}(\text{InGa})\text{Se}_2$ SOLAR CELL STRUCTURES, ARRANGED IN ORDER OF PERFORMANCE

Structure	Absorption (%)	Absorbed Power (W) (300 – 1100 nm)
300 nm CIGS SC + Silver BR	77	666
300 nm CIGS SC + Silver BR + Grating	81	690
500 nm CIGS SC + Silver BR	83	697
700 nm CIGS SC + Gold BR	85	709
700 nm CIGS SC + Silver BR	85	709
500 nm CIGS SC + Silver BR + Grating	85	711
700 nm CIGS SC + Gold BR + Grating	87	718
700 nm CIGS SC + Silver BR + Grating	87	718
AM1.5 G	100	804.8

VI. CONCLUSION

In this paper, a fundamental optical analysis framework for designing light-trapping schemes for thin-film $\text{Cu}(\text{InGa})\text{Se}_2$ solar cells was presented. The first part of the study examined the process of obtaining accurate optical material constants using a number of techniques including VASE, electromagnetic simulations, and reflectance measurements obtained using a spectrophotometer. The optical constants that were verified using all the aforementioned methods were then used to accurately develop an electromagnetic simulation tool that was subsequently used to analyze various aspects of light propagation through $\text{Cu}(\text{InGa})\text{Se}_2$ solar cells. The first aspects to be considered were the absorption and transmission characteristics of $\text{Cu}(\text{InGa})\text{Se}_2$ layers of varying thickness, thereby giving insights into the wavelengths of interest in light-trapping designs. Subsequently, the simulation tool was used to assess the reflection characteristics of different candidate materials for back surface reflectors in $\text{Cu}(\text{InGa})\text{Se}_2$ solar cells. Finally, the tool was used to analyze more complex light-trapping schemes, which included diffraction gratings, for thin, 300-, 500-, and 700-nm, $\text{Cu}(\text{InGa})\text{Se}_2$ solar cells based on superstrate cell configurations. It was found that the structures that incorporated diffraction gratings were the most effective at trapping light.

REFERENCES

- [1] J. Zhu, C. Hsu, Z. Yu, S. Fan, and Y. Cui, "Nanodome solar cells with efficient light management and self-cleaning," *Nano Lett.*, vol. 10, pp. 1979–1984, 2010.
- [2] J. G. Mutitu, S. Shi, A. Barnett, and D. W. Prather, "Hybrid dielectric-metallic back reflector for amorphous silicon solar cells," *Energies*, vol. 3, pp. 1914–1933, 2010.
- [3] J. G. Mutitu, S. Shi, C. Chen, T. Creazzo, A. Barnett, C. Honsberg, and D. W. Prather, "Thin film silicon solar cell design based on photonic crystal and diffractive grating structures," *Opt. Exp.*, vol. 16, pp. 15238–15248, 2008.
- [4] K. Orgassa, H. W. Schock, and J. H. Werner, "Alternative back contact materials for thin film $\text{Cu}(\text{In,Ga})\text{Se}_2$ solar cells," *Thin Solid Films*, vol. 431–432, pp. 387–391, May 2003.

- [5] J. Malmstrom, O. Lundberg, and L. Stolt, "Potential for light trapping in Cu(In,Ga)Se/sub 2/ solar cells," in *Proc. 3rd World Conf. Photovoltaic Energy Convers.*, May 2003, vol. 1, pp. 344–347.
- [6] W. Shafarman and J. Zhu, "Effect of substrate temperature and deposition profile on evaporated Cu(InGa)Se₂ films and devices," *Thin Solid Films*, vol. 361–362, pp. 473–477, 2000.
- [7] W. N. Shafarman, R. S. Huang, and S. H. Stephens, "Characterization of Cu(InGa)Se₂ solar cells using etched absorber layers," in *Proc. Photovoltaic Energy Convers., Conf.*, May 2006, vol. 1, pp. 420–423.
- [8] P. D. Paulson, R. W. Birkmire, and W. N. Shafarman, "Optical characterization of CuIn_{1-x}Ga_xSe₂ thin films by spectroscopic ellipsometry," *J. Appl. Phys.*, vol. 94, pp. 879–888, 2003.
- [9] P. D. Paulson, S. H. Stephens, and W. N. Shafarman, "Analysis of Cu(InGa)Se₂ alloy film optical properties and the effect of Cu off-Stoichiometry," *MRS Proc.*, vol. 865, pp. F1.1.1–F1.4.6, 2005.
- [10] S. H. Stevens, "Modeling Optical Properties of Thin Film Cu(In,Ga)Se₂ Solar Cells Using Spectroscopic Ellipsometry," Master's Thesis, Phys. Dept., Univ. Delaware, Newark, DE, USA, 2006.
- [11] R. W. Birkmire and B. E. McCandless, "Specular CuInSe₂ films for solar cells," *Appl. Phys. Lett.*, vol. 53, pp. 140–141, 1988.
- [12] J. Hilfiker, R. Synowicki, and H. G. Tompkins, "Spectroscopic Ellipsometry Methods for Thin Absorbing Coatings," in *Proc. SVC 51st Annu. Tech. Conf.*, 2008, pp. 511–516.
- [13] J. A. Woollam, B. Johs, C. Herzinger, J. Hilfiker, R. Synowicki, and C. Bungay, "Overview of variable angle spectroscopic ellipsometry (VASE), Part I: Basic theory and typical applications," in *Proc SPIE*, vol. CR72, pp. 3–28, 1999.
- [14] R. A. Synowicki, B. D. Johs, and A. C. Martin, "Optical properties of soda-lime float glass from spectroscopic ellipsometry," *Thin Solid Films*, vol. 519, no. 9, pp. 2907–2913, Feb. 28, 2011.
- [15] [Online]. Available: <http://www.jawoollam.com>
- [16] B. Johs and J. S. Hale, "Dielectric function representation by B-Splines," *Phys. Status Solidi, a*, vol. 205, no. 4, pp. 715–719, 2008.
- [17] E. D. Palik, *Handbook of Optical Constants of Solids*. New York, NY, USA: Academic, 1985.
- [18] Powerful DeltaPsi2 Software Platform drives HORIBA Scientific Ellipsometers–HORIBA. [Online]. Available: www.horiba.com. <<http://www.horiba.com/us/en/scientific/products/ellipsometers/software/>>
- [19] J. G. Mutitu, S. Shi, A. Barnett, and D. W. Prather, "Light trapping in thin silicon solar cells," presented at the 37th IEEE Photovoltaic Spec. Conf., Seattle, WA, USA, Jun. 2011.
- [20] A. C. Marsh and J. C. Inkson, "Scattering matrix theory of transport in heterostructures," *Semicond. Sci. Technol.*, vol. 1, pp. 285–290, 1986.
- [21] M. Auslender and S. Hava, "S-matrix propagation algorithm in full-vectorial optics of multilayer grating structures," *Opt. Lett.*, vol. 21, pp. 1765–1767, 1996.
- [22] D. M. Whittaker and I. S. Culshaw, "Scattering-matrix treatment of patterned multilayer photonic structures," *Phys. Rev. B*, vol. 38, pp. 2610–2618, 1999.

Authors' photograph and biographies not available at the time of publication.